Imaging of apoptosis: Tait provides an overview of recent progress toward molecular imaging agents that can detect cell death in vivo and outlines the potential for future clinical applications in diagnosis and therapy. . . . . ***Page 1573***

Dual-time PET perspective: Hicks looks at the history and significance of temporal profiling of tracer localization and previews an article in this issue of *JNM* on PET characterization of focal abnormalities remote from primary cancer sites. . . . . ***Page 1577***

Total lesion glycolysis in sarcoma: Benz and colleagues investigate whether combined assessment of tumor volume and metabolic activity improves the accuracy of ^{18}F-FDG PET for predicting histopathologic tumor response in patients with soft-tissue sarcomas.. . . . . ***Page 1579***

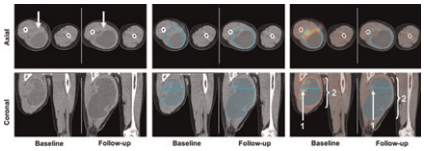

PET/CT in bronchioloalveolar carcinoma: Goudarzi and colleagues correlate CT and PET data in patients with bronchioloalveolar carcinoma or cancer of other histology to determine the contributions of the anatomic and functional components of PET/CT in differentiating lung disease. . . . . ***Page 1585***

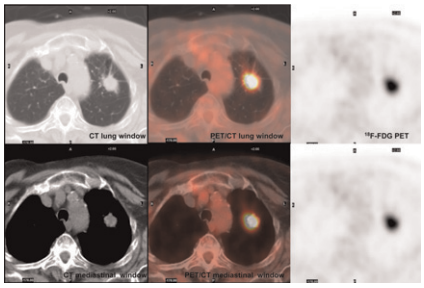

PET in head and neck cancer: Scott and colleagues report on a multicenter study exploring the effect of PET on initial management plans, staging, and treatment outcomes in patients with untreated head and neck cancer. . . . . ***Page 1593***

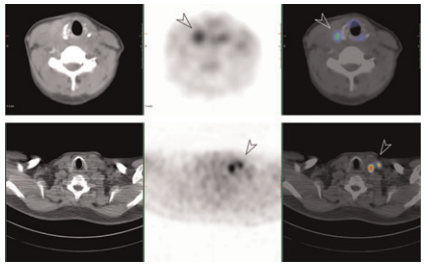

Tracer uptake in synthetic grafts: Wassélius and colleagues assess ^{18}F-FDG uptake in aortic grafts in patients with or without symptoms of graft infection and describe the risks of false-positive diagnoses in this setting. . . . ***Page 1601***

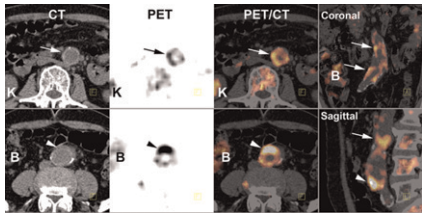

Dual-time PET in lung cancer: Uesaka and colleagues evaluate the efficacy of dual–time-point ^{18}F-FDG PET for staging lung cancer and for differentiating metastatic from nonmetastatic lung cancer lesions. . . . . ***Page 1606***

Nuclear imaging of pheochromocytoma: Ilias and colleagues compare functional imaging using ^{18}F-fluorodopamine PET, ^{123}I-MIBG scintigraphy, or somatostatin receptor scintigraphy in patients with biochemically proven nonmetastatic or metastatic pheochromocytoma. . . . . ***Page 1613***

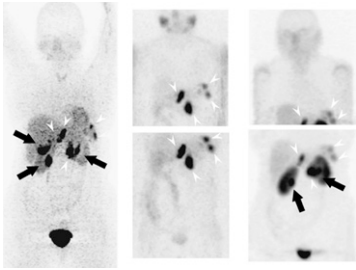

Tumor blood flow reproducibility: Lodge and colleagues report on a method quantifying the reproducibility of the ^{15}O-water technique for tumor blood flow applications and briefly outline the implications of their findings for drug development research. . . . . ***Page 1620***

nAChRs in smokers: Mukhin and colleagues describe the potential of quantitative PET imaging for elucidating the role of nicotine-induced upregulation of nicotinic acetylcholine receptors in smoking and after smoking cessation. . . . . *Page 1628*

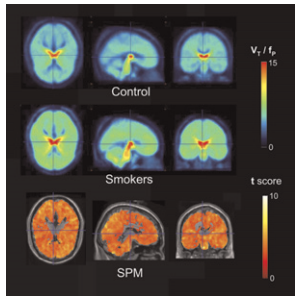

Gated myocardial SPECT and reorientation: Knollmann and colleagues assess the possibility of algorithm-specific effects related to varying heart axes as a source of error in gated SPECT. . . . . ***Page 1636***

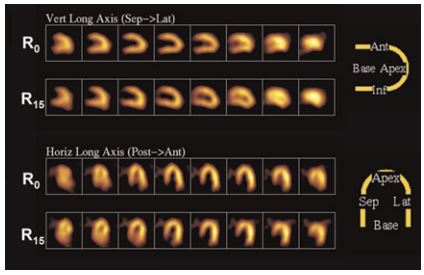

Gated ^{82}Rb PET versus CT ventriculography: Chander and colleagues compare functional parameters from gated ^{82}Rb PET with simultaneous high-resolution contrast-enhanced CT ventriculography, obtained as a byproduct of CT coronary angiography during hybrid cardiac PET/CT. . . . . ***Page 1643***

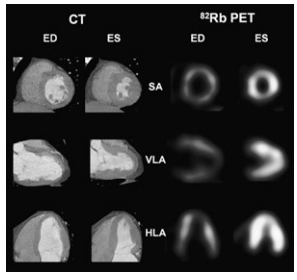

Small-animal SPECT and SPECT/CT: Franc and colleagues provide an educational overview of current technologies and advances in preclinical investigation with SPECT imaging. . . . . ***Page 1651***

Dosimetry of ^{18}F-AH111585: McParland and colleagues detail the safety, biodistribution, and internal dosimetry of a radiolabeled peptide PET tracer with a high affinity for the $\alpha_v\beta_3$ integrin receptor involved in angiogenesis. . . . . ***Page 1664***

Full-ring micro insert device: Wu and colleagues describe a prototype full-ring insert device designed to enhance image resolution in existing small-animal PET scanners. . . . . ***Page 1668***

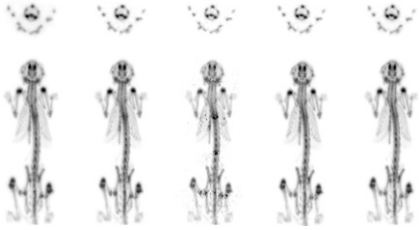

Imaging atheroma: Ishino and colleagues report on the design and preparation of ^{99m}Tc-LOX-1-mAb, a radiolabeled anti-lipoprotein receptor monoclonal IgG, and on initial animal studies of its utility as an atherosclerosis imaging agent. . . . . ***Page 1677***

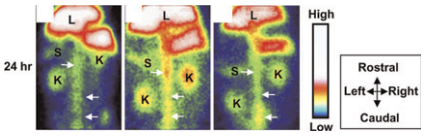

Imaging microRNA targeting: Kim and colleagues review the development and analysis of a bioluminescent reporter system for monitoring functional targeting of microRNA-221, which plays a key role in gene regulation in papillary thyroid carcinoma. . . . . ***Page 1686***

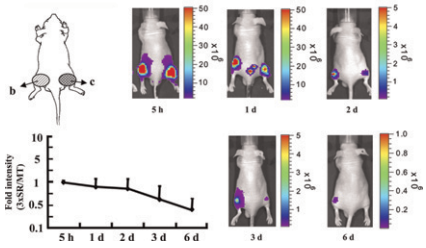

Assessment of erythropoietin cardioprotection: Doue and colleagues characterize the effect of erythropoietin on ^{99m}Tc-annexin V myocardial uptake in a rat model of ischemia and reperfusion. . . . . ***Page 1694***

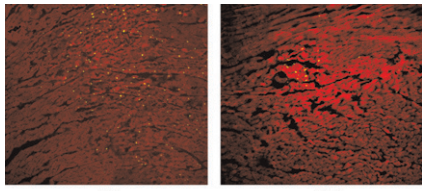

Cardiac neuropathy in diabetic mice: Kusmic and colleagues investigate in a mouse model of long-lasting type II diabetes whether the mismatch between ^{123}I-MIBG early uptake and washout is the consequence of a more generalized autonomic nervous system disorder. . . . . ***Page 1701***

Prolonged cholesterol loading and tracer uptake: Zhao and colleagues evaluate the aortic uptake of ^{18}F-FDG and ^{99m}Tc-annexin A5 in apolipoprotein E–deficient and wild-type mice placed on high-fat diets. . . . ***Page 1707***

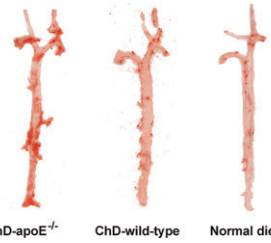

^{18}F-labeled myocardial PET tracer: Higuchi and colleagues use small-animal PET to investigate the potential of a new ^{18}F-labeled pyridazinone analog in a rat model of permanent and transient coronary occlusion. . . . . ***Page 1715***

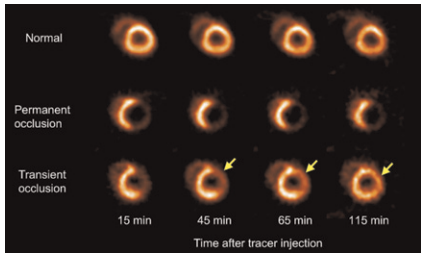

Real-time PET monitoring of RF ablation: Bao and colleagues describe preclinical investigations of the use of ^{15}O-water PET in providing real-time feedback and iterative image guidance to monitor intratumoral coverage of radiofrequency ablation therapy. . . . . ***Page 1723***

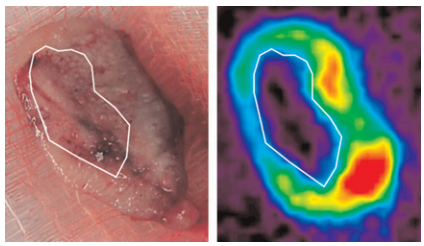

ON THE COVER

The need to study dynamic biologic processes in intact small-animal models has stimulated the development of high-resolution nuclear imaging methods. At right, small-animal SPECT/CT is applied to oncology research. In a prostate cancer xenograft model, radiolabeled antibodies for prostate-specific membrane antigen are used to monitor expression of the antigen. CT images and 3D rendering of fused images help define the tumor boundaries for more accurate image quantification.

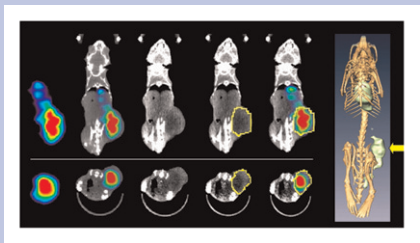

See page 1658.